Organometallics 1994, 13, 2733–2742

On Mixed Group 14–Group 14 Bonds. 8.[1] Asymmetrically Substituted Compounds $Ar_3Pb–GeAr'_3$ and $Ar_3Pb–PbAr'_3$: Comparison of Structure and Physical Behavior in the Series of Bonds Sn–Sn, Pb–Ge, Pb–Sn, and Pb–Pb[†]

Hans-Jürgen Koglin, Kerstin Behrends,[‡] and Martin Dräger*

Institut für Anorganische Chemie und Analytische Chemie der Johannes Gutenberg-Universität, D-55099 Mainz, Germany

Received December 20, 1993[⊗]

A general procedure for the synthesis of hexaarylated compounds of the type $Ar_3PbGeAr'_3$ from Ar_3PbLi and Ar'_3GeX in THF/ether at −60 °C is given. Likewise, from Ar_3PbLi and $Ar'PbI$ the asymmetrical diplumbanes $Ar_3PbPbAr'_3$ could be prepared. By the use of the bulky groups Ar and Ar′, the migration of aryl groups could be suppressed, avoiding the appearance of the mixtures $Pb_2Ar_{6-n}Ar'_n$ (n = 0–6). Nonetheless, the resulting diplumbanes $Ar_3Pb–PbAr'_3$ were always partially contaminated with some symmetric Pb_2Ar_6 and $Pb_2Ar'_6$. The structures of $(p\text{-Tol})_3PbGePh_3$ (triclinic, space group $P\bar{1}$; a = 9.983(1) b = 12.201(1) c = 15.728(2) Å; α = 95.73(1), β = 103.56(1), γ = 113.06(1)°; V = 1674(1) Å^3; Z = 2; R = 0.0434) and $(p\text{-Tol})_3PbGe(p\text{-Tol})_3$ (trigonal, space group $R\bar{3}$; a = 13.338(1), c = 36.55(1) Å; V = 5631(2) Å^3; Z = 6; R = 0.0522) have been determined. NMR chemical shifts $\delta(^{119}Sn)$ and $\delta(^{207}Pb)$ (40 compounds) and one-bond couplings $^1J(M–M')$ (16 compounds), stretching vibrations $\nu(M–M')$ and force constants $f(M–M')$ for a diatomic oscillator (38 compounds), and bond distances $d(M–M')$ (18 compounds) are compared for all six combinations M/M′ = Ge/Sn/Pb of $Ar_3M–M'Ar'_3$. Concerning the asymmetric diplumbanes $Ar_3Pb–PbAr'_3$, assignments of $\delta(^{207}Pb)$ resulted from a consideration of inductivity (comparison to $PbAr_4/Ar'_4$) and an assumed order of charge flow $\Delta(Ar \leftrightarrow Ar')$ (13 compounds). Sequences exist for $\delta(^{119}Sn)$ (Pb–Sn > Sn–Sn ≥ Sn–Ge), $\delta(^{207}Pb)$ (Pb–Pb > Pb–Sn ≈ Pb–Ge), f (Sn–Ge > Sn–Sn ≥ Pb–Sn, and Pb–Ge > Pb–Sn ≥ Pb–Pb), d (Sn–Ge ≤ Pb–Ge < Sn–Sn ≤ Pb–Sn ≤ Pb–Pb) and reduced spin–spin couplings ^1K (Pb–Sn > Sn–Sn > Pb–Pb "scatter"). The polarities $Pb^{\delta-}–Ge^{\delta+}$ and $Pb^{\delta-}–Sn^{\delta+}$ are obvious. The enhanced electronegativity of lead demonstrates the influence of its relativistically contracted 6s and 6p orbitals. With regard to $Ar_3Pb–PbAr'_3$, a relation between $^1K(Pb–Pb)$ and the charge flow $\Delta(Ar \leftrightarrow Ar')$ is indicated.

Introduction

Part 6 of our series "On Mixed Group 14–Group 14 Bonds"[2] presented a number of hexaarylethane analogues, mostly symmetrically substituted. In this work, we describe the synthesis of some asymmetric hexaaryl PbGe and PbPb compounds. Bond lengths, metal–metal vibrations, NMR chemical shifts, and spin–spin couplings are compared for a broad range of these hexaaryl compounds with Ge–Ge, Ge–Sn, Ge–Pb, Sn–Sn, Sn–Pb, and Pb–Pb cores. A recently published report similarly dealt with mixed aromatic–aliphatic substituted Ge–Sn analogues of ethane.[3]

Earlier attempts to synthesize compounds of the type $Ar_3Pb–PbAr'_3$ yielded mixtures of $Pb_2Ar_{6-n}Ar'_n$ (n = 0–6) for which all attempts of separation were unsuccessful.[4,5] An incremental method of assigning substituent effects to the ^{207}Pb NMR signals of these mixtures provided ^{207}Pb chemical shifts for all species concerned and, in addition, for the first time the directly measured values for the one-bond coupling $^1J(Pb–Pb)$.[5] These couplings range from ∓400 to ±700 Hz with a change of sign and supported an older value of 290 Hz for Pb_2Me_6 that had been obtained indirectly.[6]

Experimental Section

General Considerations. Preparations were carried out under an atmosphere of dry argon. Solvents (THF, ether) were distilled from sodium–potassium alloy. Pyridine was purified by treating 1 L of the liquid with 6 mL of bromine for 6 h and subsequently distilling (fraction 114–116 °C). Starting materials were prepared as follows: Ar_3PbLi by reaction of Ar_6Pb_2 with Li in THF,[7] Ar_3PbI by treatment of Ar_6Pb_2 with KI/I_2 (5:1) in THF,[7] $(2,5\text{-Xyl})_3PbBr$ by cleavage of $(2,5\text{-Xyl})_6Pb_2$ with Br_2 in pyridine,[8] Ph_3GeCl by redistribution of $GePh_4$ and $GeCl_4$ with $AlCl_3$ catalyst,[9] Ph_3GeBr by phenyl cleavage from Ph_4Ge with bromine

---

[†] Dedicated to Prof. Ekkehard Lindner, University of Tübingen, on the occasion of his 60th birthday. This paper includes parts of the intended Ph.D. thesis of H.-J. Koglin.

[‡] Present address: Gmelin Institut, Varrentrappstrasse 40, D-60486 Frankfurt/Main, Germany.

[⊗] Abstract published in *Advance ACS Abstracts*, May 15, 1994.

(1) Part 7: Schneider-Koglin, C.; Mathiasch, B.; Dräger, M. *J. Organomet. Chem.* **1993**, *448*, 39.

(2) Schneider-Koglin, C.; Behrends, K.; Dräger, M. *J. Organomet. Chem.* **1993**, *448*, 29.

(3) Pannell, K. H.; Párkányi, L.; Sharma, H.; Cervantes-Lee, F. *Inorg. Chem.* **1992**, *31*, 522. Cf. also: Pannell, K. H.; Kapoor, R. N.; Raptis, R.; Párkányi, L.; Fülöp, V. *J. Organomet. Chem.* **1990**, *384*, 41.

(4) Kleiner, N.; Dräger, M. *J. Organomet. Chem.* **1985**, *293*, 323.

(5) Granger, P.; Brevard, C.; Devaud, M. *J. Magn. Reson.* **1988**, *76*, 232.

(6) Kennedy, J. D.; McFarlane, W. *J. Organomet. Chem.* **1974**, *80*, C47.

(7) Willemsens, L. C.; van der Kerk, G. J. M. *J. Organomet. Chem.* **1968**, *15*, 117.

(8) Krause, E.; von Grosse, A. *Die Chemie der metall-organischen Verbindungen*; Bornträger: Berlin, 1937; p 419.

(9) Kühlein, K.; Neumann, W. P. *Justus Liebigs Ann. Chem.* **1967**, *702*, 17.

0276-7333/94/2313-2733$04.50/0

Table 1. Synthetic Results for the Pb–Ge Compounds

products $Ar_3PbGeAr'_3$	preparation init compds (Solvent; temp, °C)	yield (%), color[a]	anal.[b]				mp/dec pt (°C)[c]
			formula; M_r	C	H	Ge	
$(p\text{-Tol})_3PbGe(p\text{-Tol})_3$	$(p\text{-Tol})_3PbLi/(p\text{-Tol})_3GeBr$ (ether/THF; –60)	44, coll	$C_{42}H_{42}GePb$; 826.61	58.42 (61.03)	5.06 (5.12)	7.00 (8.78)	212/185
$(o\text{-Tol})_3PbGe(o\text{-Tol})_3$	$(o\text{-Tol})_3PbLi/(o\text{-Tol})_3GeCl$ (ether; –40)	47, coll	$C_{42}H_{42}GePb$; 826.61	57.55 (61.03)	5.17 (5.12)	(8.78)	258/258
$(o\text{-Tol})_3PbGePh_3$	$(o\text{-Tol})_3PbLi/Ph_3GeBr$ (ether/THF; –60)	36, py	$C_{39}H_{36}GePb$; 784.53	56.58 (59.71)	4.70, (4.63)	8.06[d] (9.25)	201/183
$(p\text{-Tol})_3PbGePh_3$	$(p\text{-Tol})_3PbLi/Ph_3GeCl$ (ether/THF; –60)	48, coll	$C_{39}H_{36}GePb$; 784.53	58.44 (59.71)	4.80 (4.63)	8.31 (9.25)	175/158
$(o\text{-Tol})_3PbGe(p\text{-Tol})_3$	$(o\text{-Tol})_3PbLi^-/(p\text{-Tol})_3GeBr$ (ether/THF; –60)	39, py	$C_{42}H_{42}GePb$; 826.61	58.57 (61.03)	4.93 (5.12)	6.6[d] (8.78)	187/183
$Ph_3PbGe(p\text{-Tol})_3$	$Ph_3PbLi/(p\text{-Tol})_3GeBr$ (ether/THF; –60)	26, py	$C_{39}H_{36}GePb$; 784.53	55.40 (59.71)	4.48 (4.63)	9.7[d] (9.25)	160/150
$(2,4\text{-Xyl})_3PbGePh_3$	$(2,4\text{-Xyl})_3PbLi/Ph_3GeBr$ (ether/THF; –60)	34, coll	$C_{42}H_{42}GePb$, 826.61	59.68 (61.03)	5.10 (5.12)	8.33 (8.78)	204/199

[a] Abbreviations: coll, colorless; py, pale yellow. [b] Calculated values are given in parentheses. [c] Abbreviations: mp, melting point (rapid heating); dec pt, decomposition point (precipitation of lead). [d] Impurities in Ge analysis by traces of Sb, Br, and Cl.

in CCl_4,[10] $(p\text{-Tol})_3GeBr$ analogously to Ph_3GeBr in 1,2-dibromoethane,[11] $(o\text{-Tol})_3GeCl$ by Grignard synthesis from *o*-bromotoluene and $GeCl_4$ in THF.[12] Yields are given with respect to the halide compounds used. Melting points were determined in glass capillaries in a Gallenkamp melting point apparatus (MFB-595) or in a Kofler melting block. Elemental analyses (C, H) were carried out at the Institut für Organische Chemie, Universität Mainz, with a Perkin-Elmer CHN-Analyser 240. The germanium analyses were carried out by neutron activation analysis at the Max-Planck-Institut für Chemie, Mainz, Germany, and Pb analyses by decomposition with HNO_3 and complexometric titration with titriplex III. The experimental densities of the single crystals were determined by flotation in an aqueous polytungstate solution. Solution ^{119}Sn and ^{207}Pb NMR spectra were recorded on a Bruker WP 80/DS instrument (digital resolution 0.5 Hz) at 29.88 MHz (^{119}Sn) and 16.76 MHz (^{207}Pb). The chemical shifts are relative to the external standards Me_4Sn (^{119}Sn) and Me_4Pb (^{207}Pb). Solutions of 100–200 mg of compound/3 mL of $CDCl_3$ were used.

The asymmetrically substituted diplumbanes should show two different main ^{207}Pb signals of equal intensity, corresponding to $Ar_3{}^{207}PbPbAr'_3$ and $Ar_3Pb^{207}PbAr'_3$ (22.6% natural abundance of ^{207}Pb). In addition, four signals corresponding to the AB system $Ar_3{}^{207}Pb^{207}PbAr'_3$ should appear with a joint intensity of 29% of each of the main signals. Subject to the value of $^1J(^{207}Pb–^{207}Pb)$ (lit.[5] $^1J(Ph_3PbPb(p\text{-Anis})_3)$ = 141.4 Hz, lit.[6] $^1J(Me_6Pb_2)$ = 290 Hz) the outer signals of the AB system will be weak and, depending on the distance $\Delta\delta$ between the main signals, the inner signals may not be well separated. The relative intensities 1:(0.15:0.15):1, or in the case of no resolution 1:(0.3):1, may be considerably disturbed by relaxation processes. Further, signals of the symmetric products Ar_6Pb_2 and Ar'_6Pb_2 are apparent. Figure 2 shows the two borderline cases (left, resolution of the AB system; right, no resolution).

The assignment of the two ^{207}Pb NMR chemical shifts to the lead atoms of $Ar_3Pb–PbAr'_3$ is based on the chemical shift of Pb_2Ph_6 (–79.8 ppm). This value is first corrected separately for $Ar_3{}^{207}Pb$ and $^{207}PbAr'_3$ by means of three-fourths of the difference $\delta(^{207}PbAr_4) - \delta(^{207}PbPh_4)$ (monoplumbane correction; values taken from ref 13; $\delta(^{207}Pb(2\text{-Naphth})_4)$ = –159.3 ppm). This correction can be, to a first approximation, described as an "inductive correction". A second correction will be called the "π–σ^* correction". It arises from the interaction between the aromatic groups Ar_3 or Ar'_3 with a nonbonding σ^* orbital (LUMO, relativistically lowered[34]) of the Pb–Pb bond,[14] which is in accordance with the distinct thermochromism exhibited by these slightly colored compounds. This interaction results in a charge migration between the Ar_3Pb and $PbAr'_3$ groups (the direction of migration depends on the organic substituent) and leads to a deshielding or shielding with respect to the "inductively" corrected values. By means of some trial and error, it was possible to establish a consistent order for the groups Ar and Ar′ and to assign the ^{207}Pb NMR signals of 13 asymmetric diplumbanes, 11 of which were prepared in this study and 2 of which were taken from the literature[4,5] (cf. Table 9).

Raman spectra were recorded on a SPEX 1403 spectrometer (excitation with a He/Ne laser at 633 nm and with a Kr laser at 647 nm; microcrystalline samples in capillary). Using the formula $f(M–M') = [\nu(Ar_3M–M'Ar'_3)/1303]^2[m(Ar_3M)][m(M'Ar'_3)]/[m(Ar_3M) + m(M'Ar'_3)]$ (mdyn/Å),[15] simplified force constants $f(M–M')$ were calculated (model of a diatomic oscillator). The Ar_3M groups have been treated as single nuclei.

Preparation of the Pb–Ge Compounds. Symmetrically and asymmetrically substituted Pb–Ge analogues of ethane were obtained by means of the general procedure given in eq 1. The

$$Ar_3PbLi + Ar'_3MX \underset{-60\,°C}{\overset{THF/ether}{\rightarrow}} Ar_3PbMAr'_3 + LiX \qquad (1)$$

$$M = Ge, Sn$$

results are given in Table 1. The theoretical and experimental elemental contents differ systematically. The content of carbon and germanium is too low. Only in the cases of $(p\text{-Tol})_3PbGe(p\text{-Tol})_3$ and $(p\text{-Tol})_3PbGePh_3$ could a few single crystals be obtained which were not contaminated with diplumbane. The bulk material was always contaminated in varying amounts with diplumbane. Further purification by repeated recrystallization was unsuccessful due to similar solubility behavior. Chromatographic separations were unsuccessful due to partial redistribution on the column. A detailed example follows for the symmetrical compound $(p\text{-Tol})_3PbGe(p\text{-Tol})_3$. In the asymmetric cases no ligand migration was observed.

Preparation of $(p\text{-Tol})_3PbGe(p\text{-Tol})_3$. A solution of 2.5 mmol of $(p\text{-Tol})_3PbLi$ in 7.5 mL of THF was added dropwise (1 h) into a suspension of 1.06 g (2.5 mmol) of $(p\text{-Tol})_3GeBr$ in 25 mL of ether at –60 °C. A white solid precipitated. After the addition had been completed, the stirred reaction mixture was slowly warmed to 5 °C and subsequently stored overnight at –30 °C. The mixture then was cooled to –78 °C with stirring, and the resulting precipitate was filtered off by suction. The gray-white crude product was dissolved in $CHCl_3$, and petroleum ether

---

[10] Bähr, G.; Kalinowski, H. O.; Pawlenko, S. *Houben-Weyl, Methoden der Organischen Chemie*, 4th ed.; Thieme-Verlag: Stuttgart, Germany, 1978; Vol. XIII/6, p 69.

[11] Schwarz, R.; Lewinsohn, M. *Ber. Dtsch. Chem. Ges.* **1931**, *64*, 2352.

[12] Simons, J. K.; Wagner, E. C.; Müller, J. H. *J. Am. Chem. Soc.* **1933**, *55*, 3705.

[13] Schneider-Koglin, C.; Mathiasch, B.; Dräger, M. *J. Organomet. Chem.* **1994**, *469*, 25.

[14] Pitt, C. G. *J. Organomet. Chem.* **1973**, *61*, 49. Egorochkin, A. N.; Razuvaev, G. A.; Lopatin, M. A. *J. Organomet. Chem.* **1988**, *344*, 49.

[15] Colthup, N. B.; Daly, L. H.; Wiberley, S. E. *Introduction to Infrared and Raman Spectroscopy*, 2nd ed.; Academic Press: New York, San Francisco, London, 1975; p 180.

Table 2. Synthetic Results for the Pb–Pb Compounds

products $Ar_3PbPbAr'_3$[a]	preparation init compds	yield (%)[b]	anal.[c] formula; M_r	C	H	Pb	mp/dec pt (°C)[d]
$(o\text{-Tol})_3PbPb(2,5\text{-Xyl})_3$	$(o\text{-Tol})_3PbLi/(2,5\text{-Xyl})_3PbI$	28	$C_{45}H_{48}Pb_2$; 1003.25	52.81 (53.87)	4.51 (4.82)	39.90 (41.30)	200/205
	$(2,5\text{-Xyl})_3PbLi/(o\text{-Tol})_3PbI$	31					
$(\text{m-Tol})_3PbPb(2,5\text{-Xyl})_3$	$(m\text{-Tol})_3PbLi/(2,5\text{-Xyl})_3PbBr$	10	$C_{45}H_{48}Pb_2$; 1003.25	53.48 (53.87)	4.66 (4.82)	40.13 (41.30)	120/140
	$(2,5\text{-Xyl})_3PbLi/(m\text{-Tol})_3PbI$	12					
$(p\text{-Tol})_3PbPb(2,5\text{-Xyl})_3$	$(p\text{-Tol})_3PbLi/(2,5\text{-Xyl})_3PbI$	56	$C_{45}H_{48}Pb_2$; 1003.25	53.41 (53.87)	4.51 (4.82)	40.15, (41.30)	200/195
	$(2,5\text{-Xyl})_3PbLi/(p\text{-Tol})_3PbI$	43					
$(o\text{-Tol})_3PbPb(2,4\text{-Xyl})_3$	$(2,4\text{-Xyl})_3PbLi/(o\text{-Tol})_3PbI$	57	$C_{45}H_{48}Pb_2$; 1003.25	53.97 (53.87)	4.83 (4.82)	40.05 (41.30)	203/200
$(m\text{-Tol})_3PbPb(2,4\text{-Xyl})_3$	$(m\text{-Tol})_3PbLi/(2,4\text{-Xyl})_3PbI$	61	$C_{45}H_{48}Pb_2$; 1003.25	52.39 (53.87)	4.51 (4.82)	41.16 (41.30)	127/133
$(p\text{-Tol})_3PbPb(2,4\text{-Xyl})_3$	$(2,4\text{-Xyl})_3PbLi/(p\text{-Tol})_3PbI$	49	$C_{45}H_{48}Pb_2$; 1003.25	53.32 (53.87)	4.72 (4.82)	41.08 (41.30)	200/202
	$(p\text{-Tol})_3PbLi/(2,4\text{-Xyl})_3PbI$	43					
$(2,5\text{-Xyl})_3PbPb(2,4\text{-Xyl})_3$	$(2,4\text{-Xyl})_3PbLi/(2,5\text{-Xyl})_3PbBr$	56	$C_{48}H_{54}Pb_2$; 1045.33	55.21 (55.15)	5.16 (5.21)	39.58 (39.64)	210/210
	$(2,5\text{-Xyl})_3PbLi/(2,4\text{-Xyl})_3PbI$	61					
$(2,4\text{-Xyl})_3PbPb(p\text{-Anis})_3$	$(p\text{-Anis})_3PbLi/(2,4\text{-Xyl})_3PbI$	26	$C_{45}H_{48}O_3Pb_2$; 1051.25	50.78 (51.41)	4.29 (4.60)	39.19 (39.42)	175/173
$(p\text{-Tol})_3PbPb(p\text{-Anis})_3$	$(p\text{-Anis})_3PbLi/(p\text{-Tol})_3PbI$	54	$C_{42}H_{42}O_3Pb_2$; 1009.17	49.52 (49.99)	4.00 (4.19)	40.03 (41.06)	196/192
$(2,4\text{-Xyl})_3PbPb(2\text{-Naphth})_3$	$(2\text{-Naphth})_3PbLi/(2,4\text{-Xyl})_3PbI$	23	$C_{54}H_{48}Pb_2$; 1111.35	57.04 (58.36)	4.40 (4.35)	36.07 (37.29)	198/180

[a] All asymmetric diplumbanes except $(p\text{-Tol})_3PbPb(p\text{-Anis})_3$ (colorless) are yellowish and darken reversibly on heating (thermochromism). [b] Overall yield (cf. Table 7). [c] Calculated values are given in parentheses. [d] Abbreviations: mp, melting point (start of melting; heating 2 °C/min); dec pt, decomposition point (precipitation of lead).

Table 3. Crystallographic Data and Structure Determination Details for $(p\text{-Tol})_3PbGePh_3$ and $(p\text{-Tol})_3PbGe(p\text{-Tol})_3$

	$(p\text{-Tol})_3PbGePh_3$	$(p\text{-Tol})_3PbGe(p\text{-Tol})_3$
Crystal Data (Mo $K\alpha_1$, λ = 0.709 26 Å)		
formula; M_r	$C_{39}H_{36}GePb$; 784.53	$C_{42}H_{42}GePb$; 826.61
cryst syst; space group	triclinic; $P\bar{1}$ (No. 2)	trigonal; $R\bar{3}$ (No. 148)
unit cell dimens		
a (Å), α (deg)	9.983(1); 95.73(1)	13.338(1); –
b (Å), β (deg)	12.201(1); 103.56(1)	$=a$
c (Å), γ (deg)	15.728(2); 113.06(1)	36.55(1); –
least-squares fit	124 rflns; θ = 20–22°	100 rflns; θ = 17.6–20.4°
packing: V (Å^3); Z; $F(000)$ (e)	1674(1); 2; 768	5631(2), 6, 2448
D_{calcd}, D_{exptl} (gcm^{-3})	1.56, 1.55(2)	1.46, 1.49(2)
Intensity Data Collection (Mo $K\bar{\alpha}$, λ = 0.710 69 Å, Graphite Monochromator, Temperature 22 °C)		
scan; θ range (deg); $(\sin\theta)_{max}/\lambda$ (Å^{-1})	ω; 1.5–28; 0.66	$\omega/2\theta$; 1.5–30; 0.70
range of hkl	+13,±16,±20	+18,+18,±51
ref rflns	3, every 4000 s	3, every 4000 s
loss of intensity (%) (time (days)); correcn	24.8 (9); linear	7 (6); linear
no. of rflns: measd; indep (int R)	10 273; 9729 (0.0162)	4075; 3641 (0.0210)
no. of rflns used (limit)	5427 ($I > 3\sigma(I)$)	1238 ($I > 2\sigma(I)$)
μ; abs cor	57.25; numerical by face indices	53.03; numerical by face indices
range of transmissn	0.4633–0.2062	0.6921–0.3141
Refinement		
var; ratio rflns/var; last shifts	374; 14.5; $<0.02\sigma$	67; 18.5; $<0.01\sigma$
final R; R_w	0.0434; 0.0567	0.0522; 0.0386
weight scheme w^{-1}	$\sigma^2(F) + 0.00401F^2$	$\sigma^2(F) + 0.00007F^2$
final diff Fourier max (e Å^{-3})	3.9 (near Pb)	1.06 (near Pb)

(40–60 °C) was added. To complete crystallization, this solution was stored at −30 °C overnight.

Preparation of the Pb–Pb Compounds. A 25-mL portion of a solution of Ar_3PbLi prepared from 5.7 mmol of Pb_2Ar_6 was added dropwise into a solution of 11 mmol of Ar_3PbI in 20 mL of THF at −70 °C over 2 min. While it was stirred for 4 h, the reaction mixture reached room temperature. The compounds $Ar_3PbPbAr'_3$, which are readily soluble in THF, can be fractionally precipitated by cold methanol. Slightly soluble compounds precipitate during the synthesis and should be separated by centrifugation. The remaining product can be obtained from the mother liquor as described above. For fractional recrystallization $CHCl_3$/ethanol was used. Prolonged heating and storing in solution should be avoided. The results are given in Table 2. All compounds are more or less contaminated by the symmetrical diplumbanes Pb_2Ar_6 and $Pb_2Ar'_6$ (cf. Table 9). Attempted chromatographic separation was unsuccessful due to rapid decomposition of the diplumbanes on the column.

Crystal Structure Determinations. The X-ray intensity data were collected on an Enraf-Nonius CAD4 diffractometer at 22 °C with Mo $K\alpha$ radiation (graphite monochromator). Colorless single crystals of $(p\text{-Tol})_3PbGePh_3$ were obtained by slow evaporation (desiccator, faucet slightly opened) of a cyclohexane solution (concentrated and afterwards diluted with the same amount of solvent) above solid paraffin over 4 weeks. An inclined block with dimensions 0.46 × 0.30 × 0.15 mm (triclinic faces {100}, {010}, and {001}) was used for the X-ray work. Colorless single crystals of $(p\text{-Tol})_3PbGe(p\text{-Tol})_3$ resulted upon diffusion of ligroin (40–60 °C) into a $CHCl_3$ solution (equipment and concentration as described above) for 2 days. A regular hexagonal plate with faces {100} (distance to a common origin 0.13 mm) and {001} (0.035 mm) was used for the X-ray work. The crystals were sealed in thin-walled glass capillaries. Crystal data as well as details of intensity data collection and refinement are given in Table 3. Both structures were solved by means of Patterson syntheses. The triclinic structure of $(p\text{-Tol})_3PbGePh_3$ was refined regularly: non-hydrogen atoms with anisotropic parameters and hydrogen atoms on theoretical sites riding with a common isotropic U value of 0.1052 Å^2 (aromatic hydrogen atoms) and fixed isotropic U value of 0.08 Å^2 (methyl hydrogen atoms). The trigonal structure of $(p\text{-Tol})_3PbGe(p\text{-Tol})_3$ is disordered with respect to its Pb–Ge axis, and the refinement requires some special comment.

To solve the crystal structure of $(p\text{-Tol})_3PbGe(p\text{-Tol})_3$, at first a statistical occupation (50% Pb:50% Ge) of both heavy-atom sites was assumed. With this assumption and with identical isotropic U's, all 14 independent carbon sites were found, and the first stages of refinement were carried out. Successively for

Table 4. Fractional Atomic Coordinates and Equivalent Isotropic Displacement Parameters for $(p\text{-Tol})_3PbGePh_3$ (Triclinic, $P\bar{1}$; Esd's in Parentheses)

group[a]	atom	x/a	y/b	z/c	U(eq)[b] (Å^2)
Pb(1)	Pb(1)	0.01854(3)	0.35464(2)	0.29043(2)	0.0474(1)
Ge(1)	Ge(1)	0.02159(8)	0.19347(6)	0.16643(4)	0.0445(3)
p-Tol(1)	C(11)	–0.1705(8)	0.4089(6)	0.2470(4)	0.052(3)
	C(12)	–0.2838(8)	0.3536(6)	0.1683(5)	0.060(4)
	C(13)	–0.3983(8)	0.3919(7)	0.1419(5)	0.064(4)
	C(14)	–0.4014(9)	0.4877(7)	0.1955(6)	0.064(4)
	C(15)	–0.2862(9)	0.5442(6)	0.2765(6)	0.068(4)
	C(16)	–0.1731(10)	0.5061(6)	0.3007(5)	0.065(4)
	C(17)	–0.5252(11)	0.5295(10)	0.1649(8)	0.093(7)
p-Tol(2)	C(21)	0.2249(7)	0.5322(6)	0.3407(4)	0.052(3)
	C(22)	0.3366(10)	0.5574(7)	0.4198(6)	0.074(5)
	C(23)	0.4564(10)	0.6743(9)	0.4494(6)	0.089(6)
	C(24)	0.4672(9)	0.7646(7)	0.4023(7)	0.075(5)
	C(25)	0.3579(10)	0.7362(7)	0.3237(6)	0.070(5)
	C(26)	0.2374(9)	0.6216(7)	0.2917(5)	0.062(4)
	C(27)	0.5911(12)	0.8914(9)	0.4407(10)	0.121(8)
p-Tol(3)	C(31)	–0.0100(8)	0.2753(6)	0.4083(4)	0.051(3)
	C(32)	0.0770(12)	0.2183(9)	0.4466(6)	0.086(7)
	C(33)	0.0577(14)	0.1709(11)	0.5211(7)	0.095(8)
	C(34)	–0.0522(10)	0.1758(7)	0.5588(5)	0.068(4)
	C(35)	–0.1403(10)	0.2300(8)	0.5208(5)	0.067(5)
	C(36)	–0.1208(8)	0.2796(7)	0.4476(5)	0.060(4)
	C(37)	–0.0721(13)	0.1244(9)	0.6420(6)	0.090(7)
Ph(4)	C(41)	0.0445(8)	0.2531(6)	0.0590(4)	0.049(3)
	C(42)	0.1415(10)	0.2347(7)	0.0153(5)	0.065(4)
	C(43)	0.1604(11)	0.2758(8)	–0.0626(5)	0.076(5)
	C(44)	0.0774(11)	0.3373(8)	–0.0974(6)	0.076(5)
	C(45)	–0.0226(16)	0.3548(12)	–0.0563(7)	0.109(10)
	C(46)	–0.0333(14)	0.3167(10)	0.0225(6)	0.094(8)
Ph(5)	C(51)	–0.1740(7)	0.0506(5)	0.1375(4)	0.048(3)
	C(52)	–0.2682(9)	0.0071(7)	0.0504(5)	0.070(4)
	C(53)	–0.4073(11)	–0.0931(8)	0.0297(8)	0.095(6)
	C(54)	–0.4551(10)	–0.1492(8)	0.0941(9)	0.095(7)
	C(55)	–0.3615(13)	–0.1088(9)	0.1810(9)	0.096(7)
	C(56)	–0.2188(11)	–0.0053(7)	0.2038(6)	0.076(5)
Ph(6)	C(61)	0.1905(7)	0.1517(6)	0.2126(4)	0.048(3)
	C(62)	0.3277(9)	0.2381(8)	0.2699(5)	0.067(4)
	C(63)	0.4524(10)	0.2114(10)	0.2955(7)	0.089(6)
	C(64)	0.4393(12)	0.0964(11)	0.2614(7)	0.088(7)
	C(65)	0.3046(12)	0.0110(9)	0.2057(7)	0.082(6)
	C(66)	0.1794(11)	0.0365(7)	0.1804(5)	0.070(5)

[a] Labeling as given in Figure 1 (top). [b] U(eq) = one-third of the trace of the isotropic U(*ij*) tensor.

Table 5. Fractional Atomic Coordinates and Equivalent Isotropic Displacement Parameters for $(p\text{-Tol})_3PbGe(p\text{-Tol})_3$ (Trigonal, $R\bar{3}$; Esd's in Parentheses)

group[a]	atom	x/a	y/b	z/c	U(eq)[b] (Å^2)
	Ge(1)[c]	0.00000	0.00000	0.34130(2)	0.0687(5)
Pb(1)	Pb(1)[c]	0.00000	0.00000	0.34130(2)	0.0687(5)
Ge(2)	Ge(2)[c]	0.00000	0.00000	0.41240(3)	0.0702(6)
	Pb(2)[c]	0.00000	0.00000	0.41240(3)	0.0702(6)
p-Tol(1)	C(11)	0.1669(7)	0.1157(7)	0.3173(2)	0.069(2)*
	C(12)	0.2094(7)	0.0826(7)	0.2877(2)	0.071(2)*
	C(13)	0.3164(7)	0.1572(7)	0.2726(2)	0.075(2)*
	C(14)	0.3834(7)	0.2657(8)	0.2866(2)	0.079(2)*
	C(15)	0.3446(7)	0.3011(8)	0.3161(2)	0.081(2)*
	C(16)	0.2378(7)	0.2258(7)	0.3314(2)	0.081(2)*
	C(17)	0.5003(8)	0.3498(8)	0.2696(2)	0.110(3)*
p-Tol(2)	C(21)	0.1147(7)	0.1612(7)	0.4345(2)	0.070(2)*
	C(22)	0.1040(7)	0.2582(7)	0.4257(2)	0.073(2)*
	C(23)	0.1757(7)	0.3630(7)	0.4416(2)	0.069(2)*
	C(24)	0.2590(7)	0.3803(7)	0.4658(2)	0.072(2)*
	C(25)	0.2734(7)	0.2858(7)	0.4745(2)	0.077(2)*
	C(26)	0.2018(7)	0.1793(7)	0.4590(2)	0.073(2)*
	C(27)	0.3363(8)	0.4958(8)	0.4840(2)	0.105(3)*

[a] Labeling as given in Figure 1 (bottom). [b] U(eq) = one-third of the trace of the isotropic U(*ij*) tensor; asterisks indicate isotropic *U* values. [c] Site occupation factors: Ge(1), 37% of $^1/_3$, 0.123; Pb(1), 63% of $^1/_3$, 0.21; Ge(2), 0.21; Pb(2), 0.123.

Pb and Ge, and for C, the isotropic *U*'s were changed into anisotropic thermal displacements. After each stage of refinement attempts were made to split the lead/germanium sites and/or the carbon sites. All of these attempts failed. As the thermal parameters of the heavy atoms were poorly refined, the ratio between Pb and Ge was varied by means of trial and error to optimize the difference Fourier synthesis and the parameters of the refinement. The best ratio arose at 63%:37%. Repeated attempts to refine Pb and Ge separately or to resolve the carbon sites at the 63:37 level were unsuccessful. With respect to the carbon atoms it was decided to return to isotropic *U*'s (hydrogen atoms on theoretical sites riding with a fixed isotropic *U* value of 0.08 Å^2). In order to show that the nonsymmetrical ratio was not caused by additional $Pb_2(p\text{-Tol})_6$, a Pb excess up to 20% (the experimental density of bulk material corresponds to about 13% $Pb_2(p\text{-Tol})_6$) at ratios of 50:50 and 63:37 was simulated. Both attempts did not result in better refinements, and the distributions of the maxima of the difference Fourier synthesis were worse. A test on merohedral twinning[17] also failed. It can be concluded that the chosen $(p\text{-Tol})_3PbGe(p\text{-Tol})_3$ crystal contains two identical molecules on identical sites in which 63% of the molecules are oriented in one direction of their Pb–Ge vectors and 37% in the opposite direction. The isomorphous compound $(p\text{-Tol})_3PbSn(p\text{-Tol})_3$ contains a 50%:50% distribution of two oppositely oriented Pb–Sn vectors.[16] All four compounds $(p\text{-Tol})_3$(Pb–Ge, Pb–Sn, Sn–Sn, Pb–Pb)$(p\text{-Tol})_3$ are isostructural.

For calculations and drawings local versions of SHELX-76/SHELX-86 and PLUTO-78 were respectively used in addition to several locally written routines. Calculations were performed on HB-DPS-8/70 equipment at the Zentrum für Datenverarbeitung, Universität Mainz. Tables 4 and 5 contain the final parameters.

Results

Syntheses. The syntheses of the asymmetric Pb–Pb compounds resulted in mixtures of the 3:3 diplumbanes $Ar_3PbPbAr'_3$ contaminated with varying amounts of the symmetrically substituted Pb_2Ar_6 and $Pb_2Ar'_6$, which could not be separated. Other byproducts (e.g. $Pb_2Ar_{6-n}Ar'_n$[4,5]) appeared only in trace amounts. The best solvent was found to be THF. The use of other solvents, as had been used to prepare the Pb–Ge compounds, did not give higher contents of $Ar_3PbPbAr'_3$. The optimum reaction temperature is in the range –60 to –70 °C. Above –50 °C no asymmetric compound was formed. To reduce nucleophilic attack of Ar_3Pb^- at Pb–Pb bonds,[18] it is necessary to add the Ar_3PbLi solution to the solution of Ar_3PbX. Use of a 20% excess of the halide gave the best results for the asymmetric diplumbanes. The good solubility of Ar_3PbI in THF made them the halides of choice. The reactant choice of Ar_3PbLi/Ar'_3PbI or Ar'_3PbLi/Ar_3PbI did not affect the yield.

The appearance of mixed asymmetrical diplumbanes $Pb_2Ar_{6-n}Ar'_n$ (n = 0–6) in previous work[4,5] can be explained by the transfer of single aryl groups during the reaction. The use of bulky substituents diminishes this tendency for migration in the reaction complex. However, formation of symmetrical diplumbanes cannot be fully suppressed, and especially in the case of poorly soluble compounds, symmetrical diplumbanes appear in high yield. Once formed, the asymmetrical diplumbanes are stable with

---

(16) Schneider, C.; Dräger, M. *J. Organomet. Chem.* **1991**, *415*, 349.

(17) Britton, D. *Acta Crystallogr.* **1972**, *A28*, 296. Dräger, M. Program ZWILLING; Mainz, Germany, 1989.

(18) Dräger, M.; Simon, D. *J. Organomet. Chem.* **1986**, *306*, 183.

Table 6. M–M′ Bond Lengths of Homonuclear and Heteronuclear Compounds $Ar_3M–M'Ar'_3$ (M/M′ = Ge, Sn, Pb) with Esd's in Parentheses

compds $Ar_3M–M'Ar'_3$	d(M–M′) (Å)	compds $Ar_3M–M'Ar'_3$	d(M–M′) (Å)
Ge_2Ph_6[19]	2.437(2)	$Ph_3SnGePh_3$[24]	2.606(2)[c]
Ge_2Ph_6[20]	2.446(1)	$Ph_3SnGeMe_3$[3]	2.599(3)
$Ge_2(p\text{-Tol})_6$[21]	2.423(1)	$Me_3SnGePh_3$[3]	2.652(2)
Sn_2Ph_6[22]	2.780(4), 2.759(4)[a]	$Ph_3PbGePh_3$[25]	2.623(5)[c]
$Sn_2(o\text{-Tol})_6$[2]	2.883(1)	$(p\text{-Tol})_3PbGePh_3$[d]	2.642(1)
$Sn_2(p\text{-Tol})_6$[16]	2.778(1)[b]	$(p\text{-Tol})_3PbGe(p\text{-Tol})_3$[e]	2.599(2)[c]
Pb_2Ph_6[23]	2.848(4), 2.839(4)[a]	$Ph_3PbSnPh_3$[25]	2.809(2), 2.848(2)[a]
$Pb_2(o\text{-Tol})_6$[2]	2.895(2)	$(o\text{-Tol})_3PbSn(o\text{-Tol})_3$[2]	2.845(2)[c]
$Pb_2(p\text{-Tol})_6$[16]	2.851(1)	$(p\text{-Tol})_3PbSn(p\text{-Tol})_3$[16]	2.813(2)[c]

[a] Two independent molecules. [b] Refinement of type B of two homeotypic crystal structures. [c] Statistical variation of the Sn and Ge, Pb and Ge, and Pb and Sn sites, respectively. [d] This study. Averaged values of distances and angles including C: d(Pb–C) = 2.22 Å, d(Ge–C) = 1.94 Å, ∠(C–Pb–Ge) = 113.2°, ∠(Pb–Ge–C) = 109.6°, ∠(C–Pb–C) = 105.5°, ∠(C–Ge–C) = 109.4°, t(C–Pb–Ge–C) = 59.3–60.3° (ranges of absolute torsion angles). [e] This study. Values of distances and angles including C: d(Pb–C) = 2.16 Å, d(Ge–C) = 2.08 Å, ∠(C–Pb–Ge) = 112.9(2)°, ∠(Pb–Ge–C) = 113.9(2)°, ∠(C–Pb–C) = 104.7(3)°, ∠(C–Ge–C) = 105.9(3)°, t(C–Pb–Ge–C) = 33.7, 86.3° (ranges of absolute torsion angles).

respect to migration of aryl groups and are stable in air. They are best purified by repeated recrystallization, but this procedure is restricted due to decomposition in solution and upon heating.

Crystal Structures. Figure 1 shows the molecules found ($(p\text{-Tol})_3PbGePh_3$, top; $(p\text{-Tol})_3PbGe(p\text{-Tol})_3$, bottom), and Table 6 gives the significant bond lengths and angles in comparison to similar homonuclear and heteronuclear ethane analogues with Ge–Ge, Sn–Sn, Pb–Pb, Sn–Ge, Pb–Ge, and Pb–Sn bonds.

$(p\text{-Tol})_3PbGePh_3$. The distance between Pb and Ge (2.642(1) Å) is consistent with the sum of the covalent radii of Pb (1.42 Å) and Ge (1.22 Å).[26] The Pb–C bond distances are similar to those in $Pb_2(p\text{-Tol})_6$ (d(Pb–C) = 2.20 Å[16]); the Ge–C bond distances are nearly the same as in Ge_2Ph_6 (d(Ge–C) = 1.96 Å[19]). The bond angles show the usual deviations from the tetrahedral standard, enlarged for ∠(C–M–M′) and reduced for ∠(C–M–C). This effect is small in the case of Ph_3Ge and remarkable in the case of $(p\text{-Tol})_3Pb$. Along the Pb–Ge bond axis, the aryl groups are staggered. The unit cell contains two molecules of $(p\text{-Tol})_3PbGePh_3$. The inversion center is located between them.

$(p\text{-Tol})_3PbGe(p\text{-Tol})_3$. The Pb–Ge bond distance (2.599(2) Å) is refined to a shorter value than in $(p\text{-Tol})_3PbGePh_3$. The Pb–C bond distance is found to be 0.04 Å shorter than in $Pb_2(p\text{-Tol})_6$ and the Ge–C bond distance 0.12 Å longer than in $Ge_2(p\text{-Tol})_6$, according to the 63:37 orientation of the Pb–Ge vectors in the unit cell (see Experimental Section). The C_3-symmetrical compound deviates markedly from a staggered conformation. Six molecules of $(p\text{-Tol})_3PbGe(p\text{-Tol})_3$ are arranged in the unit cell with the Pb–Ge vectors parallel to the z axis. The inversion center is located between two molecules on the 3-fold axis.

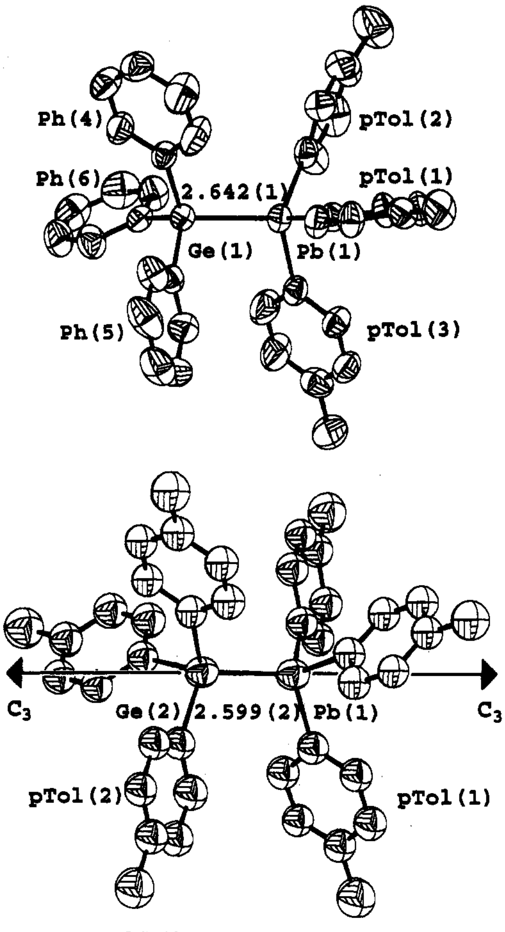

Figure 1. (Top) ORTEP drawing of the asymmetric Pb–Ge compound $(p\text{-Tol})_3PbGePh_3$ (group identifications as given in Table 4). (Bottom) ORTEP drawing of the symmetric Pb–Ge compound $(p\text{-Tol})_3PbGe(p\text{-Tol})_3$ (group identifications as given in Table 5; 3-fold axis outlined). Only one of the 63:37 statistically disordered molecules is shown. Thermal ellipsoids are at the 50% probability level.

Spectroscopic Data. Tables 7–9 give the NMR chemical shifts $\delta(^{119}Sn)$ and $\delta(^{207}Pb)$ and the Raman emissions of symmetrically and asymmetrically substituted Sn–Sn, Pb–Pb, Sn–Ge, Pb–Ge, and Pb–Sn compounds.

^{119}Sn NMR Spectroscopy. The ^{119}Sn resonances of hexaarylated compounds $Ar_3MM'Ar'_3$ (M = Sn, M′ = Ge, Sn, Pb) are shifted to high field with respect to $SnMe_4$: δ_{Sn-Ge} −164 ppm, δ_{Sn-Sn} −137 to −145 ppm, δ_{Sn-Pb} −60 to −85 ppm. Substitution of one Sn atom in a distannane by Pb causes low-field shifts of about 80 ppm. Substitution by Ge, as in the case of $Ph_3SnGePh_3$, leads to a high-field shift of about 25 ppm.

^{207}Pb NMR Spectroscopy. Analogous to the ^{119}Sn

---

(19) Dräger, M.; Ross, L. *Z. Anorg. Allg. Chem.* **1980**, *460*, 207.
(20) Dräger, M.; Ross, L. *Z. Anorg. Allg. Chem.* **1980**, *469*, 115.
(21) Roller, S. Dissertation, Mainz, Germany, 1988.
(22) Preut, H.; Haupt, H.-J.; Huber, F. *Z. Anorg. Allg. Chem.* **1973**, *396*, 81.
(23) Preut, H.; Huber, F. *Z. Anorg. Allg. Chem.* **1976**, *419*, 92.
(24) Adams, S. Dissertation, Mainz, Germany, 1987.
(25) Kleiner, N.; Dräger, M. *J. Organomet. Chem.* **1984**, *270*, 151.
(26) Huheey, J. E.; Keiter, E. A.; Keiter, R. L. *Inorganic Chemistry*, 4th ed.; Harper Collins: New York, 1993; p 292.
(27) Bulliner, P. A.; Quicksall, C. O.; Spiro, T. G. *Inorg. Chem.* **1971**, *10*, 13.
(28) Adams, S.; Dräger, M.; Mathiasch, B. *J. Organomet. Chem.* **1987**, *326*, 173.
(29) Sebald, A.; Harris, R. K. *Organometallics* **1990**, *9*, 2096.
(30) Adams, S. Diplomarbeit, Mainz, Germany, 1983.

Table 7. NMR Chemical Shifts (δ(^{119}Sn) and δ(^{207}Pb) in $CDCl_3$), Raman Emissions ν(Sn–Sn) and ν(Pb–Pb), and Force Constants *f*(Sn–Sn) and *f*(Pb–Pb) for the Symmetrically Substituted Homonuclear Compounds Sn_2Ar_6 and Pb_2Ar_6

	NMR (ppm)		Raman (cm^{-1})		force constant (mdyn/Å)	
compd	δ(^{119}Sn)	δ(^{207}Pb)	ν(Sn–Sn)	ν(Pb–Pb)	*f*(Sn–Sn)	*f*(Pb–Pb)
Sn_2Ph_6[27,28]	−144.7		138		1.9	
Sn_2(*o*-Tol)$_6$[2]	−136.8[a]		123		1.7	
Sn_2(*p*-Tol)$_6$[16]	−141.9		131		2.0	
Pb_2Ph_6[25,27,29]		−79.8		112		1.6
Pb_2(*o*-Tol)$_6$[2,29]		−88.7		103		1.5
Pb_2(*m*-Tol)$_6$		−83.5		108		1.7
Pb_2(*p*-Tol)$_6$[16]		−80.2		105		1.6
Pb_2(2,5-Xyl)$_6$		−61.2		100		1.5
Pb_2(2,4-Xyl)$_6$		−94.2		98		1.5
Pb_2(*p*-Anis)$_6$		−82.4		103		1.7
Pb_2(2-Naphth)$_6$		−74.6		87		1.3
Pb_2(1-Naphth)$_6$		−114.7[b]		109		2.1
Pb_2Mes_6[2,29]		−154.5		78		1.0

[a] Solvent: 1,1,2,2-tetrachloroethane-d_2. [b] Solvent: 1,3-dichlorobenzene (external D_2O lock).

Table 8. NMR Chemical Shifts (δ(^{119}Sn) and δ(^{207}Pb) in $CDCl_3$), Raman Emissions ν(Sn–Ge), ν(Pb–Ge), and ν(Pb–Sn), and Force Constants *f*(Sn–Ge), *f*(Pb–Ge), and *f*(Pb–Sn) for the Heteronuclear Compounds $Ar_3M–M'Ar'_3$ (M = Sn, Pb; M′ = Ge, Sn)

	NMR (ppm)		Raman (cm^{-1})			force constant (mdyn/Å)		
compd	δ(^{119}Sn)	δ(^{207}Pb)	ν(Sn–Ge)	ν(Pb–Ge)	ν(Pb–Sn)	*f*(Sn–Ge)	*f*(Pb–Ge)	*f*(Pb–Sn)
$Ph_3SnGePh_3$[30]	−163.5		150			2.2		
$Ph_3PbGePh_3$[25]		−271.5		138			2.0	
(*o*-Tol)$_3$PbGe(*o*-Tol)$_3$		−218.2		125			1.9	
(*p*-Tol)$_3$PbGe(*p*-Tol)$_3$		−270.8		137			2.2	
Ph_3PbGe(*p*-Tol)$_3$		−272.4		142			2.3	
(*o*-Tol)$_3$PbGe(*p*-Tol)$_3$		−228.0		131			2.0	
(*o*-Tol)$_3$PbGePh$_3$		−224.6		136			2.0	
(*p*-Tol)$_3$PbGePh$_3$		−269.6		137			2.1	
(2,4-Xyl)$_3$PbGePh$_3$		−225.7		131			1.9	
$Ph_3PbSnPh_3$[25]	−62.1	−256.5			125			1.8
(*o*-Tol)$_3$PbSn(*o*-Tol)$_3$[2]	−61.6[a]	−219.6[a]			114			1.7
(*p*-Tol)$_3$PbSn(*p*-Tol)$_3$[16]	−59.6	−254.2			114			1.7
(*o*-Tol)$_3$PbSnPh$_3$[2]	−85.1	−265.2			121			1.7
$Mes_3PbSnPh_3$[2]	−80.0[b]	−453.1[b]			114			1.7

[a] Solvent: 1,1,2,2-tetrachloroethane-d_2 (90 °C). [b] Solvent: benzene-d_6 (60 °C).

NMR results, the ^{207}Pb resonances are shifted to high field with respect to $PbMe_4$: δ_{Pb-Pb} −60 to −115 ppm (−155 ppm for Pb_2Mes_6), δ_{Pb-Sn} −220 to −265 ppm (−453 ppm for $Mes_3PbSnPh_3$), and δ_{Pb-Ge} −218 to −272 ppm. Substitution of one Pb atom in a diplumbane by Ge leads to high-field shifts of about 190 ppm (*o*-Tol 140 ppm). Similarly, substitution by Sn results in a high-field shift of about 175 ppm (*o*-Tol 140 ppm). As examples of the ^{207}Pb solution NMR spectra of the asymmetric Pb–Pb compounds, two spectra are shown in Figure 2 (left, (*m*-Tol)$_3$PbPb(2,5-Xyl)$_3$; right, (2,5-Xyl)$_3$PbPb(2,4-Xyl)$_3$).

From the assignments of the ^{207}Pb NMR signals of the asymmetric diplumbanes (cf. Experimental Section) arises a π–σ^* charge migration from one Ar_3Pb to $PbAr'_3$ or vice versa. The diagram in Figure 3 shows this "charge flow" from one aromatic group to the other. The heights of the columns are equivalent to a difference of differences Δ(Δδ) (difference Δδ: "experimental chemical shift" minus "monoplumbane corrected value") and visualize the direction and the relative amount of the charge flow in each of the 13 compounds. An equivalent argumentation by means of charge flow is used in ref 3 to explain differences in bond lengths.

Raman Spectroscopy. The arylated group 14 compounds show stretching vibrations ν(M–M′) of their framework below 160 cm^{-1}: ν(Pb–Pb) in a wide range from 78 to 112 cm^{-1} (mostly between 100 and 105 cm^{-1}), ν(Sn–Sn) at about 120–140 cm^{-1}, ν(Pb–Sn) between 114 and 125 cm^{-1}, ν(Pb–Ge) at 125–142 cm^{-1}, and ν(Sn–Ge) at 150 cm^{-1}. The wavenumbers of the asymmetric diplumbanes are in most cases located between the values of their symmetric homologues; the signals of the latter (byproducts, see above) appear in some cases as shoulders. To accomplish a comparison between the different stretches, the wavenumbers were corrected by the masses of the groups MAr_3 and $M'Ar'_3$. This means that a formal diatomic force constant has been calculated (cf. Experimental Section). These force constants are given in the last columns of the Tables 7–9.

Discussion

Force Constants and Chemical Shifts. Figure 4 compares the force constants with the chemical shifts δ(^{119}Sn) (top) and δ(^{207}Pb) (bottom) and visualizes the described trends. The force constants increase simultaneously with the high-field shifts of δ(^{119}Sn) and δ(^{207}Pb) NMR. These NMR chemical shifts decrease according to

$$\delta(^{119}\mathrm{Sn}):\ \mathrm{Pb{-}Sn} > \mathrm{Sn{-}Sn} \geq \mathrm{Sn{-}Ge}$$

$$\delta(^{207}\mathrm{Pb}):\ \mathrm{Pb{-}Pb} > \mathrm{Pb{-}Sn} \approx \mathrm{Pb{-}Ge}$$

All six cases are well separated in blocks. One general trend is obvious: the polarities $Pb^{\delta-}$–$Sn^{\delta+}$ and $Pb^{\delta-}$–$Ge^{\delta+}$ exist for all investigated Pb–Sn and Pb–Ge compounds. Accordingly, the thermochemical electronegativities of Pauling are in the following order: Sn, 1.96; Ge, 2.01; Pb,

Table 9. ^{207}Pb NMR Chemical Shifts (ppm; Main Signals), Couplings $^1J(^{207}Pb–^{207}Pb)$ (Hz), Raman Emissions ν(Pb–Pb) (cm^{-1}), and Force Constants f(Pb–Pb) (mdyn/Å) for the Asymmetrically Substituted Compounds Ar$_3$Pb–PbAr'$_3$

compd (content (%))[a]	NMR $\delta(^{207}Pb)$	NMR ^1J(Pb–Pb)	byproduct (content (%))[a]	Raman ν(Pb–Pb)	force constant f(Pb–Pb)
(*o*-Tol)$_3$Pb	–64.8	~0[b]	Pb$_2$(*o*-Tol)$_6$ (17)	101	1.5
(2,5-Xyl)$_3$Pb (69)	–80.6		Pb$_2$(2,5-*Xyl*)$_6$ (14)		
(*m*-Tol)$_3$Pb	–84.1	483	Pb$_2$(*m*-Tol)$_6$ (8)	104	1.6
(2,5-Xyl)$_3$Pb (92)	–74.2				
(*p*-Tol)$_3$Pb	–87.3	>200[c]		104	1.6
(2,5-Xyl)$_3$Pb (90)	–88.8		Pb(2,5-Xyl)$_3$I (10)		
(*o*-Tol)$_3$Pb	–81.4	*d*	Pb$_2$(*o*-Tol)$_6$ (20)	101	1.5
(2,4-Xyl)$_3$Pb (49)	–100.5		Pb$_2$(2,4-Xyl)$_6$ (31)		
(*m*-Tol)$_3$Pb	–92.2	>150[c]	Pb$_2$(*m*-Tol)$_6$ (21)	104	1.6
(2,4-Xyl)$_3$Pb (72)	–91.0		Pb$_2$(2,4-Xyl)$_6$ (7)		
(*p*-Tol)$_3$Pb	–97.2	*d*		101	1.5
(2,4-Xyl)$_3$Pb (36)	–105.3		Pb$_2$(2,4-Xyl)$_6$ (64)		
(2,5-Xyl)$_3$Pb	–74.6	>500[c]	Pb$_2$(2,5-Xyl)$_6$ (22)	96	1.4
(2,4-Xyl)$_3$Pb (71)	–77.3		Pb$_2$(2,4-Xyl)$_6$ (7)		
(2,4-Xyl)$_3$Pb	–113.4	*d*	Pb$_2$(2,4-Xyl)$_6$ (61)	102	1.6
(*p*-Anis)$_3$Pb (34)	–89.4		Pb$_2$(*p*-Anis)$_6$ (5)		
(*p*-Tol)$_3$Pb	–90.1	*e*	Pb$_2$(*p*-Tol)$_6$ (20)	104	1.6
(*p*-Anis)$_3$Pb (60)	–72.2		Pb$_2$(*p*-Anis)$_6$ (20)		
(2,4-Xyl)$_3$Pb	–90.6	>1000[c]		94	1.4
(2-Naphth)$_3$Pb (100)	–87.0				
(*p*-Tol)$_3$Pb	–71.9	256	Pb$_2$(*p*-Tol)$_6$ (40)	110	1.6
Ph$_3$Pb[f] (21)	–88.0		Pb$_2$Ph$_6$ (39)		
Ph$_3$Pb	–98.2	141	*g*		
(*p*-Anis)$_3$Pb[h]	–63.3				
(*o*-Tol)$_3$Pb	–76.1	*d*	*g*		
(*p*-Tol)$_3$Pb[h]	–90.5				

[a] Percentage of the integral ^{207}Pb NMR intensities (no correction). [b] No coupling visible: inner signals of the AB system coincide with the strong main signals. [c] Inner signals of the AB system not resolved: lower limit of ^1J estimated for a resolution of 2 Hz (four points of the digital resolution). [d] No coupling visible: low intensity of the whole spectrum. [e] No coupling visible: inner signals of the AB system possibly beside the bases of the byproducts (^1J(Pb–Pb) ≈ 1270 Hz). [f] Synthesis[4] optimized. [g] Mixture of all possible derivatives Ar$_{6-n}$PbPbAr'$_n$ (n = 0–6).[4,5] [h] ^{207}Pb values from refs 4 and 5; assignment as in the other cases of the table.

2.33.[31] Without doubt, the electronegativity of Pb is distinctly higher than those of Sn and Ge. A differentiation between Ge and Sn by means of the data of Figure 4 alone is not possible.[2,32]

The ranges of the force constants, calculated using the model of a diatomic oscillator (see above), are

$$f(\text{Sn–Ge})\ (2.2) > f(\text{Sn–Sn})\ (1.7–2.0) \geq f(\text{Pb–Sn})\ (1.7–1.8)$$

$$f(\text{Pb–Ge})\ (1.9–2.3) > f(\text{Pb–Sn})\ (1.7–1.8) \geq f(\text{Pb–Pb})\ (1.3–1.7)$$

$$f(\text{Br–Br})\ (2.1) \geq f(\text{I–Br})\ (2.0) > f(\text{I–I})\ (1.6)$$

For comparison, the last line gives the force constants of some halogens.[33]

The enhanced electronegativity of lead clearly demonstrates the influence of its relativistically contracted 6s and 6p orbitals.[34] No such clearcut influence can be concluded for the force constants (relativistic increase of their values[34]). The scatter of the chemical shifts and of the force constants shows that other influences are of simultaneous importance, e.g. a charge flow as demonstrated in Figure 3.

Three compounds are omitted from the bottom part of Figure 4: Mes$_3$PbSnPh$_3$, because of its high-field shift in the ^{207}Pb NMR (–453.1 ppm), and Pb$_2$Mes$_6$ and Pb$_2$(1-Naphth)$_6$, because of low (1.0 mdyn/Å) or high (2.1 mdyn/Å) force constants. Concerning Mes$_3$PbSnPh$_3$, a charge flow from the SnPh$_3$ group to the lead atom should be assumed in addition to the "inductive" effect of the "electropositive Sn atom" discussed above. This charge flow is a strong support for the chemical shift assignments of Table 9 and the order of charge flow in Figure 3: the

---

(31) Allred, A. L. *J. Inorg. Nucl. Chem.* **1961**, *17*, 215.

(32) Charissé, M.; Mathes, M.; Simon, D.; Dräger, M. *J. Organomet. Chem.* **1993**, *445*, 39.

(33) Weidlein, J.; Müller, U.; Dehnicke, K. *Schwingungsfrequenzen I Hauptgruppenelemente*; Thieme-Verlag: Stuttgart, Germany, New York, 1981; pp 56, 73.

(34) Pyykkö, P. *J. Organomet. Chem.* **1982**, *232*, 21. Pyykkö, P. *Relativistic Theory of Atoms and Molecules, A Bibliography 1916–1985*; Springer-Verlag: Berlin, 1986. Pyykkö, P. *Chem. Rev.* **1988**, *88*, 563. For a recent general discussion of the influences of relativistically contracted 6s and 6p orbitals cf.: Norrby, L. J. *J. Chem. Educ.* **1991**, *68*, 110. For an analogous behavior of the group 15 atoms neighboring tin and lead (electronegativity of Sb 2.05 and of Bi about 2.3) cf.: Bräu, E.; Falke, R.; Ellner, A.; Beuter, M.; Kolb, U.; Dräger, M. *Polyhedron* **1994**, *13*, 365.

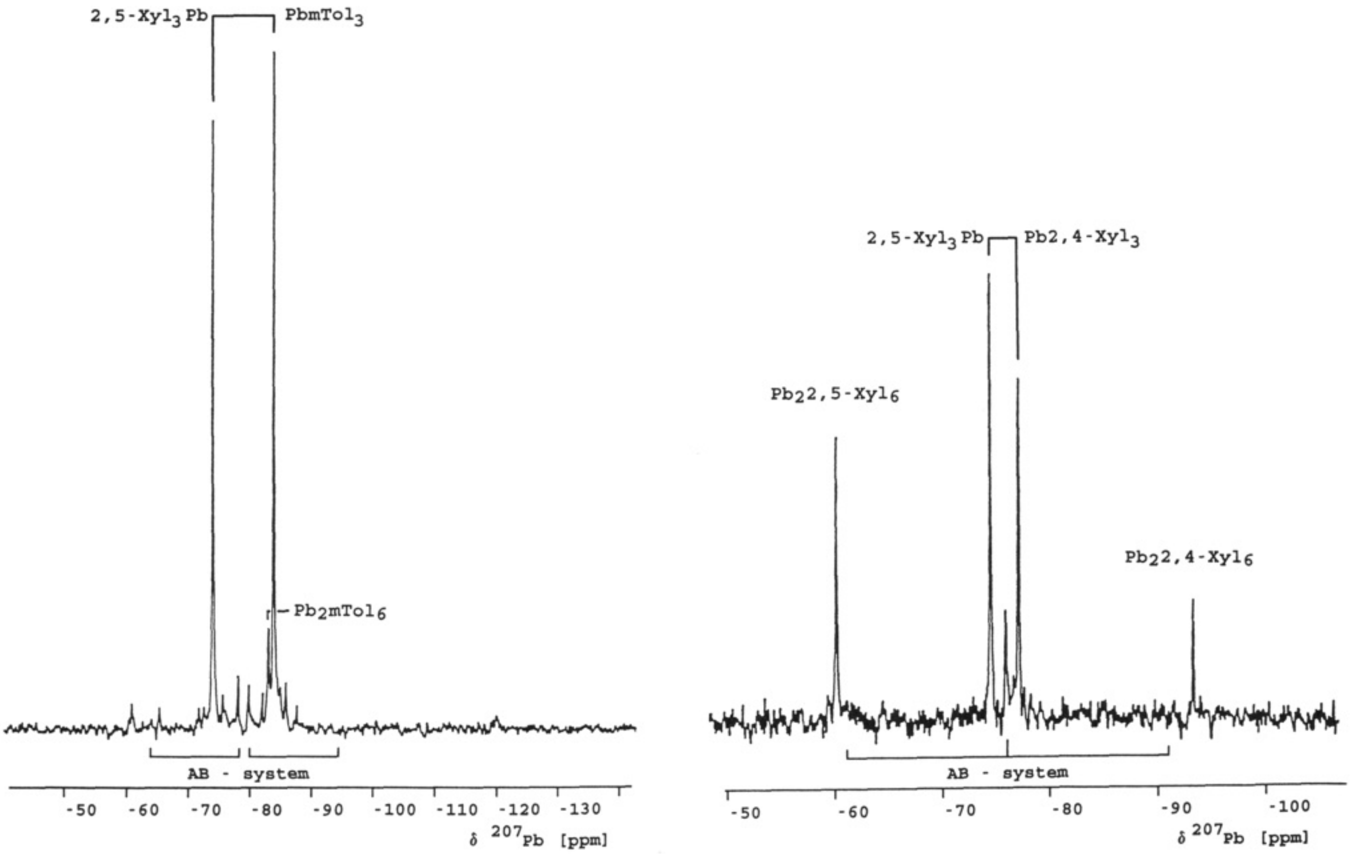

Figure 2. ^{207}Pb NMR of the asymmetric Pb–Pb compounds (m-Tol)$_3$PbPb(2,5-Xyl)$_3$ (left) and (2,5-Xyl)$_3$PbPb(2,4-Xyl)$_3$ (right).

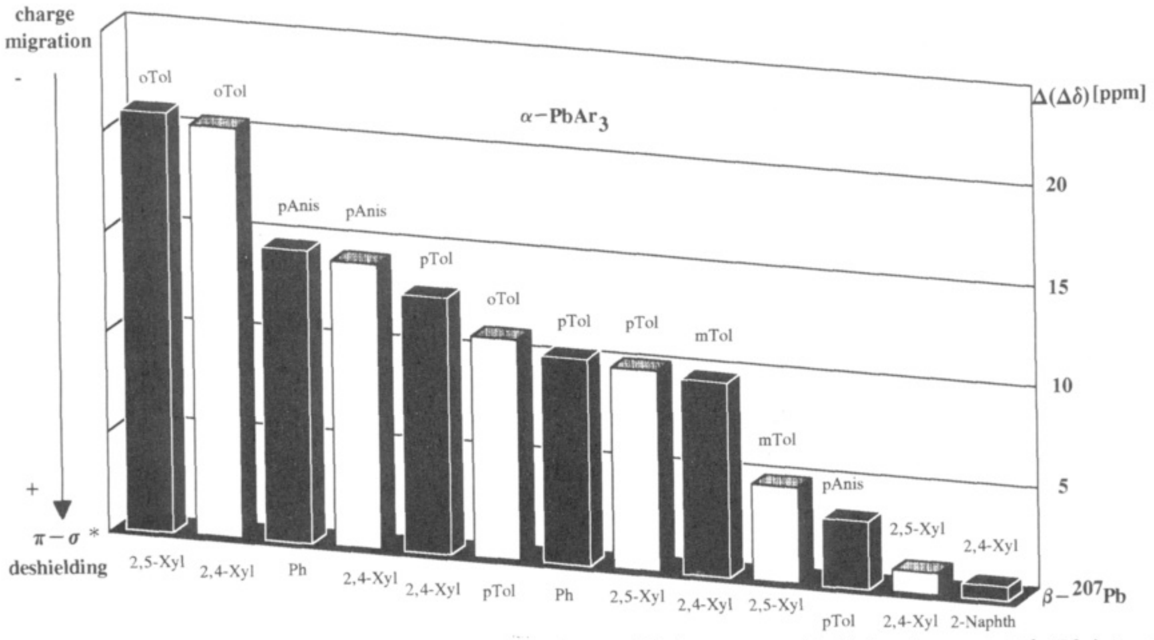

Figure 3. π–σ^* deshielding of β-^{207}Pb by aromatic groups Ar at α-Pb in asymmetric diplumbanes Ar_3Pb–$PbAr'_3$ with regard to the chemical shift of α-^{207}Pb. $\Delta(\Delta\delta)$ is defined as the difference of experimental minus the corrected value differences (correction of Ar_3Pb and $PbAr'_3$ by means of monoplumbane shifts with $PbPh_4$ and Pb_2Ph_6 as standards).

charge flow from the phenyl to the mesityl group adds a large column to the left side of the graph in Figure 3.

The two compounds Pb_2Mes_6 and Pb_2(1-Naphth)$_6$ are omitted from Figure 4 due to their extreme force constants; the ^{207}Pb NMR chemical shifts of both are also the most high field shifted of all diplumbanes investigated (−154.5 and −114.7 ppm). This indicates an overall charge flow from the aromatic groups into the σ^* LUMO's of the lead–lead bond. The three cases Pb_2(2-Naphth)$_6$ (−74.6 ppm), Pb_2(2,5-Xyl)$_6$ (*o,m*-disubstituted, −61.2 ppm), and Pb_2(2,4-Xyl)$_6$ (*o,p*-disubstituted, −94.2 ppm) exhibit the most low field resp. high field shifts of the other eight diplumbanes of Table 7. The extreme high-field shift of Pb_2Mes_6 (*o,p,o*-trisubstituted, −154.5 ppm) marks a continuation of the *o,p*-disubstituted case. In accordance with the low force constant of Pb_2Mes_6, the σ^* LUMO is clearly

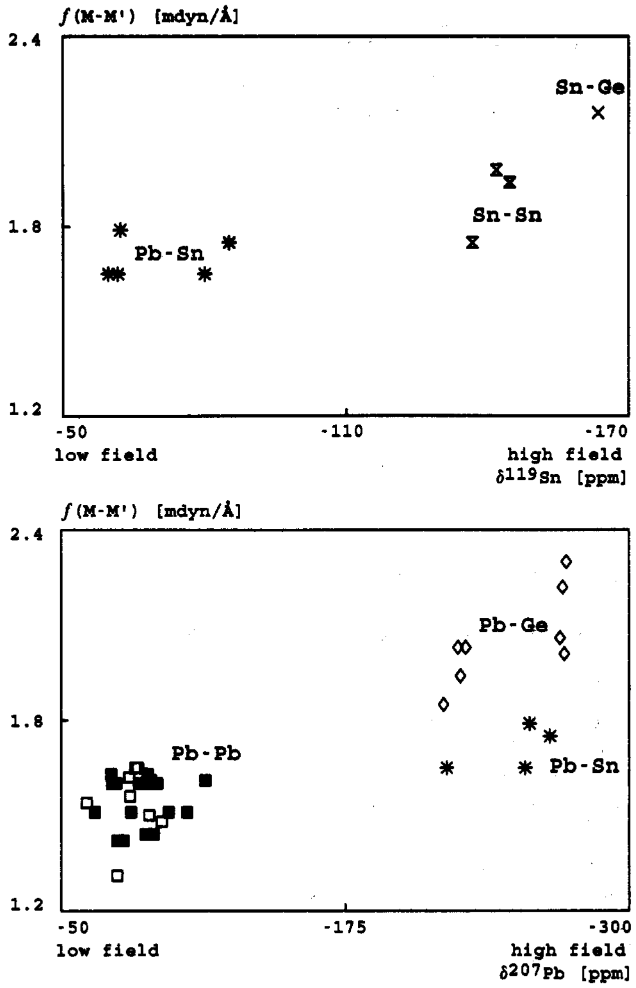

Figure 4. Plots of force constants f(M–M′) calculated from Raman wavenumbers (M/M′ = Ge, Sn, Pb) versus the chemical shifts $\delta(^{119}Sn)$ (top; δ scale Δ = 120 ppm) and $\delta(^{207}Pb)$ (bottom; δ scale Δ = 250 ppm; shaded squares indicate asymmetric $Ar_3PbPbAr'_3$ compounds). The following compounds are omitted from the ^{207}Pb part of Figure 4 (bottom): Pb_2(1-Naphth)$_6$ ($\delta(^{207}Pb)$ −114.7 ppm, f(Pb–Pb) = 2.1 mdyn/Å); Pb_2Mes_6 ($\delta(^{207}Pb)$ −154.5 ppm, f(Pb–Pb) = 1.0 mdyn/Å); $Mes_3PbSnPh_3$ ($\delta(^{119}Sn)$ −80.0 ppm, $\delta(^{207}Pb)$ −453.1 ppm, f(Pb–Sn) = 1.7 mdyn/Å).

lowered. The nearly colorless solution of this compound in xylene changes reversibly to violet when heated to boiling. The high-field shift of Pb_2(1-Naphth)$_6$ ("*o*"-substitution) is in contrast with the low-field shifts of the "*m*"-substituted cases Pb_2(2-Naphth)$_6$ and Pb_2(2,5-Xyl)$_6$. The high force constant of Pb_2(1-Naphth)$_6$ results possibly only from the mode of its force constant calculation, in which the heavy Pb(1-Naphth)$_3$ groups have been chosen as point masses.

Force Constants and Bond Distances. Figure 5 displays the force constants f(M–M′) versus the bond distances d(M–M′) of symmetrically substituted compounds (phenyl, *p*-tolyl, and *o*-tolyl as substituents). The distances are in the order

$$d(\text{Sn–Ge}) \le d(\text{Pb–Ge}) < d(\text{Sn–Sn}) \le d(\text{Pb–Sn}) \le d(\text{Pb–Pb})$$

In each series, the force constants follow the bond lengths roughly in an opposite direction. The partial relative short Pb–Sn and Pb–Pb distances demonstrate the relativistically contracted 6s and 6p orbitals of lead.[34]

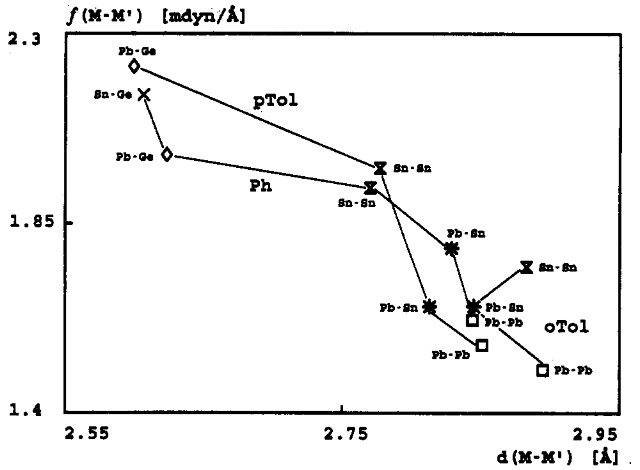

Figure 5. Plot of force constants f(M–M′) calculated from Raman wavenumbers versus distances d(M–M′) (M/M′ = Ge, Sn, Pb) for three symmetrically substituted series of compounds.

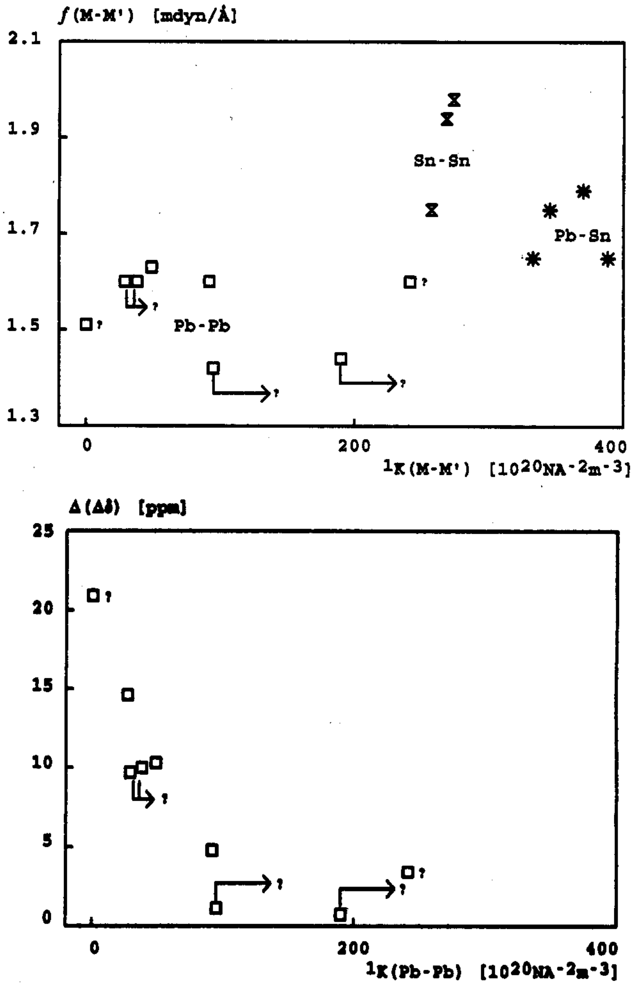

Figure 6. Plots of force constants f(M–M′) (mdyn/Å) (top for Pb–Pb, Sn–Sn, and Pb–Sn compounds; calculated from Raman wavenumbers) and of charge migration $\Delta(\Delta\delta)$ (ppm) (bottom for Pb–Pb compounds; from Figure 3) versus the reduced coupling constants ^1K(M–M′). Symbols with a question mark are uncertain to some extent; for symbols marked with an arrow, only the lower limit of ^1K(Pb–Pb) could be determined.

Spin–Spin Couplings. Figure 6 (top) compares the force constants with the reduced coupling constants of the one-bond spin–spin couplings ^{119}Sn–^{119}Sn, ^{207}Pb–

Table 10. Coupling Constants ^1J(M–M′) (Hz), Reduced Coupling Constants[a] ^1K(M–M′) (10^{20} N A^{-2} m^{-3}), and Force Constants f(M–M′) (mdyn/Å) for Compounds with Sn–Sn, Pb–Sn, and Pb–Pb Bonds

	coupling constant			reduced coupling constant			force constant		
compd	^1J(Sn–Sn)	^1J(Pb–Sn)	^1J(Pb–Pb)	^1K(Sn–Sn)	^1K(Pb–Sn)	^1K(Pb–Pb)	f(Sn–Sn)	f(Pb–Sn)	f(Pb–Pb)
Sn_2Ph_6[27,28]	4480			268.48			1.94		
Sn_2(*o*-Tol)$_6$[2]	4297			257.51			1.75		
Sn_2(*p*-Tol)$_6$[16]	4570			273.87			1.98		
$Ph_3PbSnPh_3$[25]		3469			370.36			1.79	
(*p*-Tol)$_3$PbSn(*p*-Tol)$_3$[16]		3640			388.62			1.65	
(*o*-Tol)$_3$PbSn(*o*-Tol)$_3$[2]		3119			332.99			1.65	
(*o*-Tol)$_3$PbSnPh$_3$[2]		3236			345.49			1.75	
(*p*-Tol)$_3$PbPbPh$_3$			256			48.69			1.63
(*m*-Tol)$_3$PbPb(2,5-Xyl)$_3$			483			91.87			1.60
Ph$_3$PbPb(*p*-Anis)$_3$[5]			141			26.82			*b*
(*o*-Tol)$_3$PbPb(2,5-Xyl)$_3$[d]			0			0			1.51
(*p*-Tol)$_3$PbPb(2,5-Xyl)$_3$[d]			>200[c]			>38[c]			1.60
(*m*-Tol)$_3$PbPb(2,4-Xyl)$_3$[d]			>150[c]			>29[c]			1.60
(2,5-Xyl)$_3$PbPb(2,4-Xyl)$_3$[d]			>500[c]			>95[c]			1.42
(2,4-Xyl)$_3$PbPb(2-Naphth)$_3$[d]			>1000[c]			>190[c]			1.44
(*p*-Tol)$_3$PbPb(*p*-Anis)$_3$[d]			1270			241.56			1.60

[a] $(4\pi^2/h\gamma_M\gamma_{M'})^1J$(M–M′) according to ref 35. [b] No Raman data. [c] Lower limit. [d] ^{207}Pb–^{207}Pb couplings are uncertain to some extent.

^{119}Sn, and ^{207}Pb–^{207}Pb; the values are given in Table 10. The Pb–Pb squares designated with a question mark are uncertain to some extent with respect to their coupling constants. The Sn–Sn and Pb–Sn compounds are located in a narrow range according to reduced couplings and to force constants (^1K(Pb–Sn) > ^1K(Sn–Sn)). In contrast, the force constants and, even more, the reduced couplings of the Pb–Pb compounds scatter. For ^1K(Pb–Pb) a possible change in sign is discussed in the literature only on the basis of a very limited amount of data.[5,34] Figure 6 (bottom) shows the charge migration $\Delta(\Delta\delta)$ in ppm (cf. Figure 3) versus the reduced coupling constants ^1K(Pb–Pb) of the asymmetrically substituted Pb–Pb compounds in Table 10. The charge migration decreases with increasing values of the reduced coupling constants. A related dependence of the force constants from ^1K remains uncertain. On the assumption of a change of sign of the coupling constants,[5,34] a bell-shaped curve would result with high charge migration at zero coupling and a decrease at high positive or negative values of the reduced couplings.

Conclusion

The overall sequences of NMR chemical shifts, reduced couplings, force constants, and bond lengths given are clear. Yet, when the substituents are varied, values differ along each series with the same kinds of nuclei (cf. Figure 1: *d*(Pb–Ge) = 2.642 and 2.599 Å). Obviously, the three effects mentioned—inductive polarities between the heavy atoms M/M′, inductivities between Ar/Ar′ and M/M′, and the charge flow Ar ↔ Ar′—are connected (partly parallel and partly counteracting). Thus, it was not possible to resolve all inconsistencies for the 44 compounds given in Tables 6–9 by means of simple one-dimensional reasoning. The latter was used successfully in the literature for explaining the bond length difference of the pair Ph_3Sn–$GeMe_3$/Me_3Sn–$GePh_3$ (2.599/2.652 Å).[3] Generally, a thorough multidimensional consideration is needed by using data from specially "tailored" compounds.

Acknowledgment. We thank the Deutsche Forschungsgemeinschaft, Bonn-Bad Godesberg, Germany, and the Fonds der Chemischen Industrie, Frankfurt/Main, Germany, for financial support.

Supplementary Material Available: Tables listing anisotropic displacement parameters, H atom positional parameters, all bond lengths and bond angles, and torsion angles for (*p*-Tol)$_3$PbGePh$_3$ and (*p*-Tol)$_3$PbGe(*p*-Tol)$_3$ (6 pages). Ordering information is given on any current masthead page.

OM930856V

---

(35) Pople, J. A.; Santry, D. P. *Mol. Phys.* **1964**, *8*, 1.